October, 1980] © *1980 The Chemical Society of Japan* *Bull. Chem. Soc. Jpn.*, **53**, *2809—2814 (1980)* 2809

Nuclear Magnetic Resonance in Hemihydrate Gypsum

Kenji Shimomura, Toshikazu Nagashima,† Akira Sanjoh,††
Makoto Yoshida,†† and Hisao Negita*,††
Department of Physics, Faculty of Integrated Arts and Sciences, Hiroshima University,
Higashisenda-machi, Hiroshima 730
†*Ube Research Center, Central Glass Co., Ltd., Okiube, Ube 755*
††*Department of Chemistry, Faculty of Science, Hiroshima University, Higashisenda-machi, Hiroshima 730*

(Received January 12, 1980)

The proton spin-lattice relaxation times T_1 and T_{1D} along the static and dipolar magnetic fields have been measured at 18 MHz for the water molecule in powdered hemihydrate gypsum $CaSO_4\cdot(1/2)H_2O$. The minima of T_1 and T_{1D} were observed at $10^3/T=4.3$(233 K) and 7.0(143 K) respectively. These are ascribed to the 180° flip motion of water molecules, with an activation energy of 15.1 kJ/mol. At higher temperatures, the translational diffusion of water molecules becomes dominant; this is not observed in gypsum $CaSO_4\cdot 2H_2O$. The activation energy of this motion is estimated to be 32.2 kJ/mol. In hemihydrate gypsum, though the diffusion is supposed to be anisotropic, the jumping distance of the water molecule is tentatively examined by Torrey's lattice diffusion theory.

In the series of crystal forms of gypsum $CaSO_4\cdot nH_2O$, two kinds of hemihydrate gypsum, $CaSO_4\cdot(1/2)H_2O$, are known. These are called α- and β-hemihydrate gypsum, and are obtained with different methods of preparation. The NMR method has been applied by several workers to investigate the internal motions of water molecules in gypsum. Holcomb and Pedersen[1)] measured the spin-lattice relaxation time T_1 in gypsum over a wide temperature range, and showed that the relaxation is dominated by the 180° flip motion which modulates the interactions with protons on neighboring water molecules. Look and Lowe[2)] examined the rotating frame spin-lattice relaxation time $T_{1\rho}$. Jeener *et al.*[3,4)] evaluated the 180° flips of water molecules in gypsum and pointed out the additional relaxation due to infrequent, thermally activated jumps of water molecules at high temperatures.

It is interesting to consider the difference between the crystal structures of gypsum and hemihydrate gypsum, in which the nuclear motion affects the magnetic resonance linewidth and relaxation times. The crystal structure of gypsum consists of layers parallel to the (010) plane. The layers are bound together by bonds from water molecules, which link the Ca^{2+} ion and O atom of a $SO_4{}^{2-}$ ion in one layer with an O atom of $SO_4{}^{2-}$ in the adjacent layer.[5,6)] A number of studies have been done on the crystal structure of hemihydrate gypsum.[7–11)] The space group of the trigonal unit cell is $P3_221$ and the cell dimensions are $a=b=6.83$ Å, $c=12.70$ Å, $\gamma=120°$, and $Z=6$. These results indicate that the characteristic features of hemihydrate gypsum are due to the existence of tunnels (or systems of interconnected cavities) which serves as the passage of the water molecules through the c-axis; water molecules are held together in these tunnels, with the closest neighboring O–O distance of water molecules being 4.23 Å. Accordingly, the motion of the water molecule in hemihydrate gypsum seems to have more degrees of freedom than that in gypsum. In hemihydrate gypsum, no fundamental difference of the crystal structure has been found between α- and β-hemihydrate gypsum.[12,13)] But Lasis suggests that β-hemihydrate gypsum contains more lattice defects than α-hemihydrate gypsum.[14)]

Differential thermal analysis was performed in order to distinguish the α- and β-hemihydrate gypsum; this proved to be superior to the X-ray powder diffraction method. These two methods, however, gave little information on the internal motions of water molecules. Therefore, the NMR experiment was performed in order to obtain a valuable check on the motions of the water molecules. Both pulse and cw methods were employed on the powdered α- and β-hemihydrate gypsum, and the spin-lattice relaxation times T_1 along the static, T_{1D} along the dipolar magnetic fields, and the second moments were measured to examine the motion of water molecules in hemihydrate gypsum.

Experimental

The proton relaxation time T_1 was measured at 18 MHz by the solid echo method, because the free-induction decay signals were so weak in hemihydrate gypsum. T_{1D} was obtained by the 90°-45°-45° pulse method. In order to do the on-line measurement, the free decay on an oscilloscope was amplitude-to-time converted (ATC) and measured by a digital counter, while the pulse interval was measured by

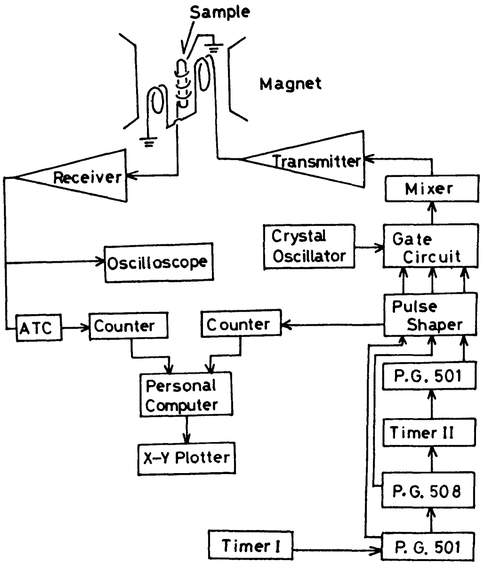

Fig. 1. Block diagram of the pulse NMR spectrometer.

another counter. These results were displayed on an X-Y plotter through a PC-7200 computer. A block diagram of the pulse NMR spectrometer is shown Fig. 1. The resonance-line-shape curve was measured at 40 MHz using a JEOL model JES-BE-1. The samples are powdered gypsum and hemihydrate gypsum from commercial sources. Three kinds of samples, K-α, P-α, and O-β, named after the makers and types of hemihydrate gypsum, were used for the experiment. A sample of hemihydrate gypsum which had been kept for about 47 h at 10^{-2}—10^{-3} Torr** was also examined. In this case, preparation was performed at about 0 °C, with care to avoid the evacuation of the water of crystallization.[15]

Results and Discussion

Second Moment. Figure 2 shows the temperature dependence of the second moments in hemihydrate gypsum. The second moments in K-α, P-α, and O-β are 24 G^2,** 25 G^2, and 23 G^2 at 123 K respectively, and the gypsum value is 30 G^2 at 173 K. This fact shows the distance between the protons in the hemihydrate gypsum is larger than that in the gypsum. But, as shown in Fig. 2, the second moments at 123 K have not reached their rigid lattice values, so we will not discuss further these values of the second moments. It is seen in Fig. 2 that the second moments of raw hemihydrate gypsum decrease suddenly above room temperature and have a minimum value (*ca.* 13 G^2) at 330 K. This remarkable anomaly is pronounced in K-α, whereas the same decrease is not observed in the evacuated hemihydrate gypsum. Recovery of the second moment occurs gradually above 330 K in the raw samples, and the curve becomes similar to that of the evacuated samples. Above 383 K the second moments decrease in the same way for both raw and evacuated hemihydrate gypsum.

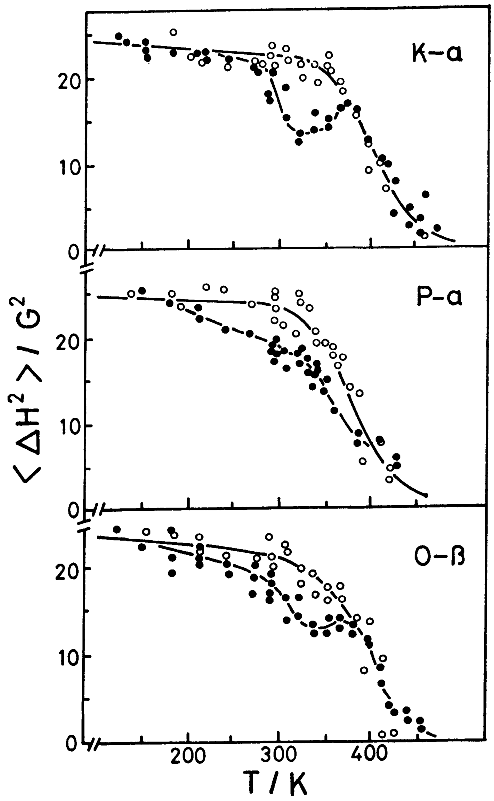

Fig. 2. Second moments of the proton resonance lines in K-α, P-α, and O-β as a function of temperature.
●: Raw samples, ○: evacuated samples.

Fig. 3. Absorption derivative curves in the raw and evacuated hemihydrate gypsum at room temperature. (a) Raw samples, (b) evacuated for about 47 h at 10^{-2}—10^{-3} Torr.

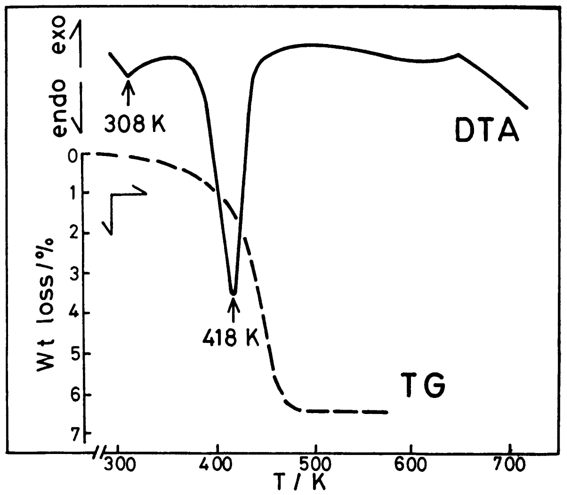

Fig. 4. DTA and TG curves in raw O-β.
Solid line indicates the DTA curve and dashed line TG curve.

Figure 3 shows the derivative curves of absorption spectra in raw and evacuated hemihydrate gypsum at room temperature; the difference in the central parts is important. It is obvious that the central part of the spectra, which is characterized by the diffusing adsorption waters, is remarkable in raw O-β, compared with both raw K-α and P-α. In an effort to explain the anomaly in the second moment at around 330 K, the thermal properties of hemihydrate gypsum were examined. Figure 4 shows the DTA and TG curves of O-β. The endothermic peaks at 308 K and 418 K correspond to dehydration of adsorption water and water of crystallization respectively. In hemihydrate

---

** Throughout this paper 1 Torr=133.322 Pa and 1 G=10^{-4} T.

gypsum, adsorption water seems to be held on the surface as well as in the crystal lattice. When the temperature is higher than 290 K, the adsorption water molecules in the raw sample diffuse in the crystal lattice and leave from its surface, so that the motional-narrowing of the resonance line due to diffusion appears and contributes to the central part of the resonance line, resulting in the decrease of the second moment. The recovery of the second moment above 330 K in the raw sample can be ascribed to the exhaustion of the diffusing adsorption water molecules in the crystal, which restores the second moment back to that of the evacuated sample which has less mobile water molecules. The decrease of the second moment above 383 K seems to be ascribed to the diffusion of the water molecule due to the dehydration of rigidly bound water, which agrees well with the results of the DTA and TG curves.

Spin-lattice Relaxation Time. The spin-lattice relaxation times T_1 and T_{1D} *vs.* inverse temperature in gypsum are shown in Fig. 5, in which $(T_1)_{min}$($\approx$90 ms) appears at $10^3/T=4.0$(250 K) and $(T_{1D})_{min}$($\approx$1 ms) is expected to be present at $10^3/T=7.0$—8.0(143—125 K). The observed T_1 curve below 250 K gives the activation energy of 24.7 kJ/mol; we found $T_1\approx 3T_{1D}$ on the higher temperature side of $(T_1)_{min}$. The relaxation times as a function of temperature are also shown for the three kinds of hemihydrate gypsum in Fig. 6. In hemihydrate gypsum, $(T_1)_{min}$ appears at $10^3/T=4.3$(233 K) and $(T_{1D})_{min}$ at $10^3/T=7$(143 K). These two minima are ascribed to the same mechanism. $(T_1)_{min}$ at $10^3/T=4.3$ are 0.8, 1, and 1.4 s in O-β, K-α, and P-α respectively. On the higher temperature side of $(T_1)_{min}$, T_1 decreases rapidly; this is not observed in gypsum. This tendency is seen also in T_{1D} curves. It may be concluded that $(T_1)_{min}$ may exist at $10^3/T=2.5$—2.6(*ca.* 390 K) with the value of 0.1—0.2 s, if we take the value of $(T_{1D})_{min}$ at $10^3/T$ to be 3.5(286 K). The temperature dependence of T_1 and T_{1D} in evacuated O-β is shown in Fig. 7. It is obvious from Fig. 7 that T_1 and T_{1D} of the evacuated sample are longer than those of the raw sample.

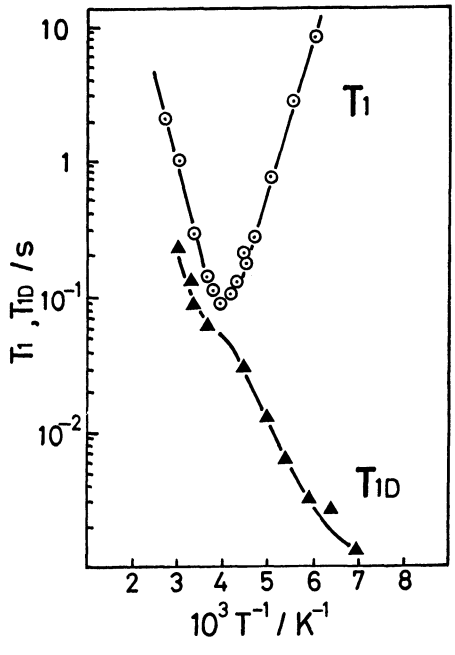

Fig. 5. Temperature dependence of the proton T_1 and T_{1D} in powdered gypsum $CaSO_4\cdot 2H_2O$.

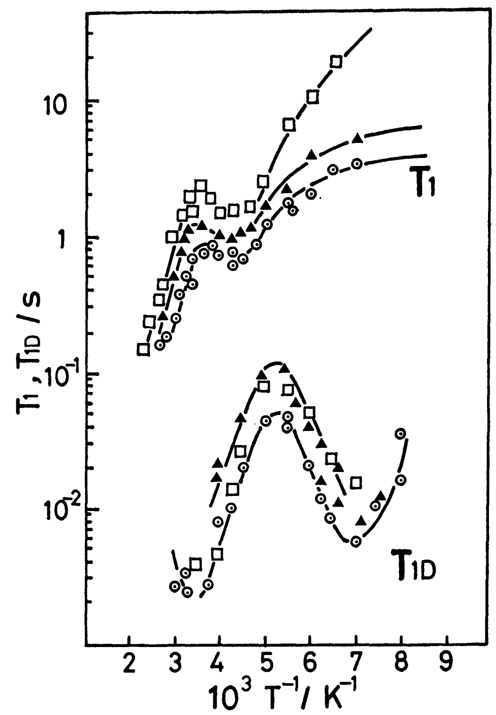

Fig. 6. Temperature dependence of the proton T_1 and T_{1D} in powdered hemihydrate gypsum $CaSO_4\cdot(1/2)$-H_2O.

⊙: O-β, ▲: K-α, □: P-α.

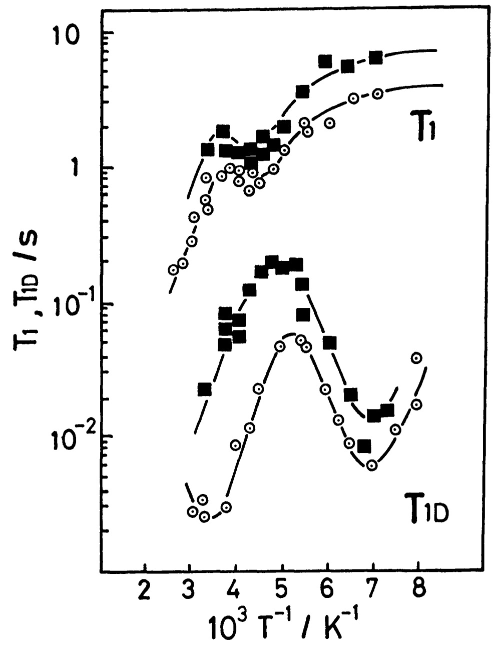

Fig. 7. Temperature dependence of the proton T_1 and T_{1D} in the evacuated O-β. Relaxation times in raw O-β are also shown.

⊙: Raw sample, ■: evacuated sample.

At temperatures lower than 182 K, the T_1 *vs.* $1/T$ curve has a small gradient. This shows that the relaxation rate due to paramagnetic impurities predominates in this temperature region, which is important in O-β and K-α but not in P-α. Therefore, the observed relaxation time $(T_1)_{\mathrm{obsd}}$ can be expressed as:

$$\frac{1}{(T_1)_{\mathrm{obsd}}} = \frac{1}{(T_1)_{\mathrm{e}}} + \frac{1}{(T_1)_{\mathrm{n}}}, \tag{1}$$

where $1/(T_1)_{\mathrm{e}}$ is the relaxation rate due to paramagnetic impurities and $(T_1)_{\mathrm{n}}$ is the relaxation time due to other sources. In Fig. 8 $(T_1)_{\mathrm{n}}$ were plotted after the contribution of the paramagnetic impurities was removed. In Fig. 8 we obtain $(T_1)_{\mathrm{min}}=1$, 1.4, and 1.6 s for O-β, K-α, and P-α respectively, and 1.5 s for evacuated O-β.

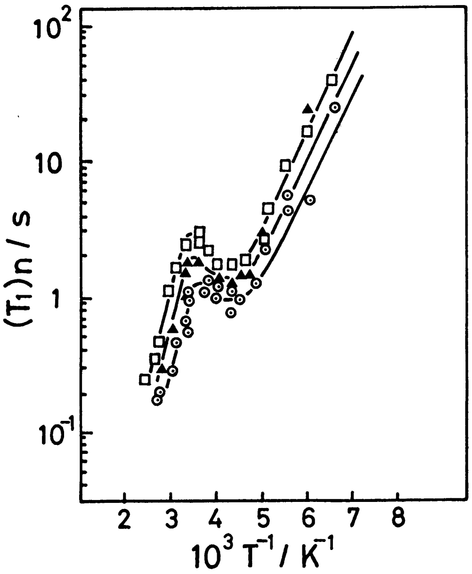

Fig. 8. Temperature dependence of the T_1 in hemihydrate gypsum. Contribution due to paramagnetic impurity is subtracted from the observed T_1 values. ⊙: O-β, ▲: K-α, □: P-α.

The proton relaxation time may be associated with two types of molecular motions: (1) the 180° flip of a water molecule about the bisector of the H–O–H angle, and (2) the translational diffusion of the water molecules. Since the intramolecular dipole-dipole interaction Hamiltonian is invariant to 180° flip motion, the intramolecular interaction makes no contribution to T_1, for which only the intermolecular interactions are responsible. The value of the second moment, which mainly comprises the intramolecular interaction, is not affected by the flip motion. Thus, as shown in Fig. 2, the observed second moment of the evacuated sample does not change appreciably up to the temperature of dehydration. Accordingly, we assign the 180° flip process to the low temperature $(T_1)_{\mathrm{min}}$. The spin-lattice relaxation time T_1 due to this flipping is given by[2,16]

$$\frac{1}{T_1} = \gamma^4\hbar^2\frac{3I(I+1)}{16N}\sum_{i\neq j}\left[B_{ij}^{(1)}\frac{\tau_c}{1+(1/4)\omega_0{}^2\tau_c{}^2}\right.$$
$$\left.+(2A_{ij}^{(1)}+B_{ij}^{(2)})\frac{\tau_c}{1+\omega_0{}^2\tau_c{}^2}+2A_{ij}^{(2)}\frac{\tau_c}{1+4\omega_0{}^2\tau_c{}^2}\right], \tag{2}$$

where the notation is that of Ref. 16. Equation 2 at $\omega_0\tau_c \gg 1$ gives

$$\frac{1}{T_1} = \frac{C}{\omega_0 N\tau_c}, \tag{3}$$

where the constant C includes the proton-proton distances between water molecules. We obtained 15.1 kJ/mol for the activation energy E_a from $(T_1)_{\mathrm{n}}$ data in Fig. 8 by assuming the relation $\tau_c=\tau_c{}^0\exp(E_a/RT)$. This value is identical to that obtained from the observed $T_{1\mathrm{D}}$. The slight difference of T_1 values between α- and β-hemihydrate gypsum may be due to the amount of water molecules in the crystal lattice.

We next turn to the effect of translational diffusion on T_1 in the hemihydrate gypsum. No theoretical treatment of the diffusion has been done on a non-cubic crystal. Assuming a homogeneous distribution of nuclear dipoles, Bloom[17] obtained T_1 for the case of self-diffusion as follows:

$$\frac{1}{T_1} = \frac{8\pi}{5}\gamma^4\hbar^2 I(I+1)N$$
$$\times\int_a^\infty r^{-4}\left\{\frac{\tau_c}{1+\omega_0{}^2\tau_c{}^2}+\frac{4\tau_c}{1+4\omega_0{}^2\tau_c{}^2}\right\}dr, \tag{4}$$

where N is the number of diffusing spins per unit volume and a is the distance of the closest approach of pairs of nuclei. It follows from the crystal data of hemihydrate gypsum that $N=1.17\times10^{22}/\mathrm{cm}^3$. At the $(T_1)_{\mathrm{min}}$ where $\omega_0\tau_c=0.62$, the following Eq. 5 is obtained from Eq. 4[18]

$$\frac{1}{(T_1)_{\mathrm{min}}} = \frac{6\pi}{5}\gamma^4\hbar^2 N\frac{0.475}{\omega_0 a^3}. \tag{5}$$

Substituting $\tau_c=r^2/12D$[19] on the lower temperature side where $\omega_0{}^2\tau_c{}^2 \gg 1$, an asymptotic form is obtained from Eq. 4 as follows:

$$\frac{1}{T_1} = \frac{144\pi}{25}\gamma^4\hbar^2 ND\frac{1}{\omega_0{}^2 a^5}, \tag{6}$$

where D is the diffusion coefficient and can be expressed as $D_0\exp(-E_a/RT)$. On the higher temperature side where $\omega_0{}^2\tau_c{}^2 \ll 1$, we also obtain

$$\frac{1}{T_1} = \gamma^4\hbar^2 N\frac{\pi}{2Da}. \tag{7}$$

In order to examine the common features for both BPP (Bloembergen, Purcell, and Pound) and Torrey's theories, we consider the case where three-dimensional isotropic diffusion occurs in a space lattice. T_1 due to this motion is given for $I=1/2$ as follows:[20]

$$\frac{1}{T_1} = \frac{9}{8}\gamma^4\hbar^2\{S_1(\omega)+4S_1(2\omega)\}, \tag{8}$$

where S_1 is the spectral density of the random time function. In the limiting case $\langle r^2\rangle \gg a^2$, for which the mean flight distance is long, we obtain

$$S_1(\omega) = \frac{8\pi N}{45a^3}\left\{\frac{\tau}{1+(\omega\tau/2)^2}\right\}. \tag{9}$$

Then T_1 is given by

$$\frac{1}{T_1} = \frac{2\pi N}{5a^3}\gamma^4\hbar^2\left\{\frac{\tau/2}{1+(\omega\tau/2)^2}+\frac{2\tau}{1+(\omega\tau)^2}\right\}, \tag{10}$$

where the correlation time τ_c is equal to $\tau/2$.

At a temperature which satisfies the relation $\omega\tau=1.23$, Eq. 10 gives a $(T_1)_{\min}$

$$\frac{1}{(T_1)_{\min}}=\frac{2\pi N}{5a^3}\gamma^4\hbar^2\frac{1.425}{\omega}=\frac{6\pi N}{5}\gamma^4\hbar^2\frac{0.475}{\omega a^3},\quad(11)$$

which agrees well with Eq. 5. In general, when the correlation time is short ($\omega_0{}^2\tau_c{}^2\ll1$), Torrey's theory agrees well with the BPP theory.20) On the other hand, where $\omega_0{}^2\tau_c{}^2\gg1$, the former theory provides a much better fit than the latter. But, as shown in Eqs. 5 and 11, both theories give the same $(T_1)_{\min}$ so that we can estimate the parameters a and D from this region.

In O-β, $(T_1)_{\min}$ is estimated to be about 0.16 s at $10^3/T=2.25$; we obtain $a=2.56$ Å from Eq. 5 or 11. Distance a changes from 2.45 Å to 2.67 Å, if $(T_1)_{\min}$ is taken from 0.14 to 0.18 s. If we put Eq. 6 equal to Eq. 7, we have an approximate condition at the $(T_1)_{\min}$18) and we obtain

$$D=\sqrt{\frac{25}{288}}\omega_0a^2.\quad(12)$$

From this equation $a=2.56$ Å yields $D=2.1\times10^{-8}$ cm²/s. On the other hand, we found the activation energy $E_a=32.2$ kJ/mol for diffusion from T_1 in Fig. 6 and the constant D_0 was then obtained to be 4.28×10^{-4} cm²/s. In Fig. 9, the straight line indicates the calculated relaxation time T_1 which is followed by Eq. 6.

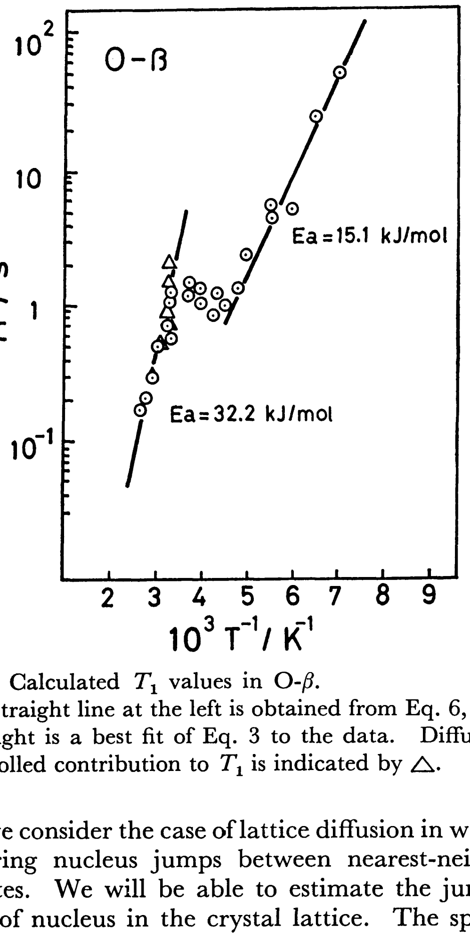

Fig. 9. Calculated T_1 values in O-β.
The straight line at the left is obtained from Eq. 6, and the right is a best fit of Eq. 3 to the data. Diffusion controlled contribution to T_1 is indicated by △.

Now we consider the case of lattice diffusion in which a spin-bearing nucleus jumps between nearest-neighbor lattice sites. We will be able to estimate the jumping distance of nucleus in the crystal lattice. The spectral density $S_1(\omega)$ is given by21)

$$S_1(\omega)=\frac{8c}{15\omega^2\tau}\sum_i\frac{1}{r_i{}^6}\left\{1-\frac{1}{z}\sum_j\left(\frac{r_i}{r_j}\right)^3\left(1-\frac{3l^2}{2r_j{}^2}\sin^2\Theta_j\right)\right\},\quad(13)$$

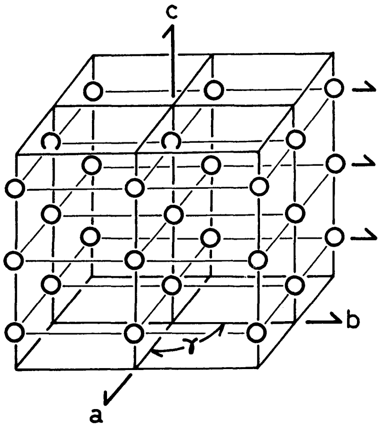

Fig. 10. The crystal structure of hemihydrate gypsum. Positions of water molecules are shown by large circles. Cell dimensions of the trigonal unit cell are $a=b=$ 6.83 Å, $c=12.70$ Å, $\gamma=120°$, and $Z=6$.

where Θ_j is the angle between proton-proton vectors $\boldsymbol{r}_j$ and $\boldsymbol{r}_i$, z is the number of the nearest neighbors of a lattice site, and c is the ratio of the number of nuclei to the number of lattice sites. In a water molecule, we let $c=2$ as a rough estimation.22) Figure 10 shows the positions of water molecules in hemihydrate gypsum. In order to estimate the jumping distance l, we substitute the distance r for l. Then Eq. 13 becomes

$$S_1(\omega)=\frac{124}{15\omega^2\tau}l^{-6}.\quad(14)$$

Next we evaluate the value of T_1 for two cases, that is, $l=4.23$ Å (closest O–O bond distance between the water molecules along the c-axis) and 6.83 Å (the corresponding distance on a horizontal plane). In the former case

$$S_1(\omega)=1.437\times10^{45}\frac{1}{\omega^2\tau}\quad(15)$$

and

$$\frac{1}{T_1}=3.234\times10^{45}\frac{\gamma^4\hbar^2}{\omega^2\tau}=4.81\times10^8D,\quad(16)$$

whereas for the latter case

$$S_1(\omega)=8.144\times10^{43}\frac{1}{\omega^2\tau}\quad(17)$$

and

$$\frac{1}{T_1}=1.832\times10^{44}\frac{\gamma^4\hbar^2}{\omega^2\tau}=1.05\times10^7D,\quad(18)$$

in which $\tau=l^2/6D$ is applied. For example, at $10^3/T=$ 3.0 and $D=3.82\times10^{-9}$ cm²/s, we obtain $T_1=0.5$ s for $l=4.23$ Å and 25 s for $l=6.83$ Å. The observed value is about 0.3 s. Moreover, since $D=9.85\times10^{-10}$ cm²/s at $10^3/T=3.35$, we obtain $T_1=2.1$ s for $l=4.23$ Å and $T_1=96$ s for $l=6.83$ Å. The observed T_1 is about 2 s. It is obvious from these results that the lattice diffusion model for $l=4.23$ Å agrees better with the experimental value.

Conclusion

The investigation of the proton magnetic resonance spectra and its relaxation times of hemihydrate gypsum has lead to the following conclusions:

1) β-Hemihydrate gypsum contains more adsorption water in the crystal lattice than α-hemihydrate gypsum.

2) It is found that the 180° flip of the water molecule ($E_a=15.1$ kJ/mol) already begins at the temperature below 125 K which is the lower temperature limit of the T_{1D} measurement. In raw samples, the adsorption water which combines loosely with the crystal lattice is released at about room temperature. The translational diffusion of the water molecule ($E_a=32.2$ kJ/mol) begins in the crystal lattice above the temperature of 200 K, and results in the dehydration of the water of crystallization at about 380 K.

3) In O-β, we obtain $D_0 \approx 4\times10^{-4}$ cm^2/s and the distance of closest approach of the water molecules $a\approx2.6$ Å. Applying 4.23 Å as the jumping distance of the water molecule between the lattice points in Torrey's theory, we can explain the observed T_1 values above 286 K successfully.

References

1) D. F. Holcomb and B. Pedersen, *J. Chem. Phys.*, **36**, 3270 (1962).

2) D. C. Look and I. J. Lowe, *J. Chem. Phys.*, **44**, 2995 (1966).

3) H. Eisendrath, W. Stone, and J. Jeener, *Phys. Rev. B*, **17**, 47 (1978).

4) H. Eisendrath and J. Jeener, *Phys. Rev. B*, **17**, 54 (1978).

5) M. Atoji and R. E. Rundle, *J. Chem. Phys.*, **29**, 1306 (1958).

6) W. F. Cole and C. J. Lancucki, *Acta Crystallogr., Sect. B*, **30**, 921 (1974).

7) P. Gallitelli, *Per. Min.*, **4**, 1 (1933).

8) O. W. Flörke, *Neues Jahrb. Mineral. Abh.*, **84**, 189 (1952).

9) P. Gay, *Min. Mag.*, **35**, 354 (1965).

10) F. G. Berschadski and O. P. Mtschedlow-Petrossian, *Zh. Prikl. Khim.*, **1966**, 1449.

11) O. P. Mtschedlow-Petrossian and F. G. Berschadski, *Silikattechnik*, **18**, 147 (1967).

12) H. Lehmann, *Tonind. Ztg.*, **91**, 6 (1967).

13) H. Miyazaki and N. Takagi, *Kogyo Kagaku Zasshi*, **73**, 1766 (1970).

14) A. Yu. Lasis, *Stroit. Mat.*, **1**, 38 (1971).

15) J. J. Gardet, B. Guilhot, and M. Soustelle, *Bull. Soc. Chim. Fr.*, **1970**, 3377.

16) K. Sagisawa, H. Kiriyama, and R. Kiriyama, *Bull. Chem. Soc. Jpn.*, **51**, 1942 (1978).

17) M. Bloom, *Physica*, **23**, 767 (1957).

18) G. W. Smith, *J. Chem. Phys.*, **36**, 3081 (1962).

19) D. F. Holcomb and R. E. Norberg, *Phys. Rev.*, **98**, 1074 (1955).

20) A. Abragam, "The Principles of Nuclear Magnetism," Oxford University Press, London (1961).

21) H. C. Torrey, *Phys. Rev.*, **92**, 962 (1953).

22) D. C. Look, I. J. Lowe, and J. A. Northby, *J. Chem. Phys.*, **44**, 3441 (1966).